Title
Genetic engineering in primary human B cells with CRISPR-Cas9 ribonucleoproteins.

Authors
Wu, Chung-An M
Roth, Theodore L
Baglaenko, Yuriy
et al.

Publication Date
2018-06-01

DOI
10.1016/j.jim.2018.03.009

Peer reviewed

Journal of Immunological Methods 457 (2018) 33–40

Contents lists available at ScienceDirect

Journal of Immunological Methods

journal homepage: www.elsevier.com/locate/jim

Research paper

Genetic engineering in primary human B cells with CRISPR-Cas9 ribonucleoproteins

Chung-An M. Wu[a,1], Theodore L. Roth[b,1], Yuriy Baglaenko[h,i,1,2], Dario M. Ferri[h,i], Patrick Brauer[i,j], Juan Carlos Zuniga-Pflucker[i,j], Kristina W. Rosbe[f], Joan E. Wither[h,i,k,***], Alexander Marson[b,c,d,e,**], Christopher D.C. Allen[a,g,*]

[a] Cardiovascular Research Institute, Sandler Asthma Basic Research Center, 555 Mission Bay Blvd S, University of California, San Francisco, San Francisco, CA 94143, USA
[b] Department of Microbiology and Immunology, 513 Parnassus Ave, University of California, San Francisco, CA 94143, USA
[c] Department of Medicine, Diabetes Center, Helen Diller Family Comprehensive Cancer Center, 513 Parnassus Ave, University of California, San Francisco, CA 94143, USA
[d] Innovative Genomics Institute, 2151 Berkeley Way, University of California, Berkeley, Berkeley, CA 94720, USA
[e] Chan Zuckerberg Biohub, 499 Illinois St, San Francisco, CA 94158, USA
[f] Department of Otolaryngology, 550 16th St, University of California, San Francisco, San Francisco, CA 94143, USA
[g] Department of Anatomy, 555 Mission Bay Blvd S, University of California, San Francisco, San Francisco, CA 94143, USA
[h] Krembil Research Institute, 60 Leonard Ave, University Health Network, Toronto, Ontario, Canada
[i] Department of Immunology, 60 Leonard Ave, University of Toronto, Toronto, Ontario, Canada
[j] Sunnybrook Research Institute, 2075 Bayview Ave, University of Toronto, Toronto, Ontario, Canada
[k] Department of Medicine, 60 Leonard Ave, University of Toronto, Toronto, Ontario, Canada

ARTICLE INFO

Keywords:
CRISPR-Cas9
Cas9 ribonucleoprotein
Primary human B cells
Genome engineering

ABSTRACT

Genome editing in human cells with targeted nucleases now enables diverse experimental and therapeutic genome engineering applications, but extension to primary human B cells remains limited. Here we report a method for targeted genetic engineering in primary human B cells, utilizing electroporation of CRISPR-Cas9 ribonucleoproteins (RNPs) to introduce gene knockout mutations at protein-coding loci with high efficiencies that in some cases exceeded 80%. Further, we demonstrate knock-in editing of targeted nucleotides with efficiency exceeding 10% through co-delivery of oligonucleotide templates for homology directed repair. We delivered Cas9 RNPs in two distinct in vitro culture systems to achieve editing in both undifferentiated B cells and activated B cells undergoing differentiation, reflecting utility in diverse experimental conditions. In summary, we demonstrate a powerful and scalable research tool for functional genetic studies of human B cell biology that may have further applications in engineered B cell therapeutics.

1. Introduction

The ability to genetically manipulate human cells provides immense opportunity for research and therapeutic applications (Lombardo and Naldini, 2014). The engineered nuclease CRISPR-Cas9 has revolutionized the ability to generate targetable knockout and knock-in genomic edits, facilitating mechanistic genetic studies directly in primary human cells, which is critical for understanding medically relevant biology that may not be conserved in model organisms (Barrangou and Doudna, 2016). Recent studies also provide pre-clinical evidence for the potential of CRISPR in therapeutic applications, such as disruption of the hepatitis B virus (Zhen et al., 2015), prevention of muscular dystrophy via germline DNA editing in a mouse model (Long et al., 2014), correction of a CFTR gene defect in intestinal stem cell organoids cultured from cystic fibrosis patients (Schwank et al., 2013), and skin transplantation of human epidermal progenitor cells

* Correspondence to: Christopher D.C. Allen, Cardiovascular Research Institute, Sandler Asthma Basic Research Center, and Department of Anatomy, University of California, San Francisco, 555 Mission Bay Blvd S, San Francisco, CA 94143, USA.
** Correspondence to: Alexander Marson, Department of Microbiology and Immunology, Department of Medicine, Diabetes Center, and Helen Diller Family Comprehensive Cancer Center, University of California, San Francisco, 513 Parnassus Ave, San Francisco, CA 94143, USA.
*** Correspondence to: Joan E. Wither, Krembil Research Institute, University Health Network, 60 Leonard Ave, Toronto, Ontario M5T 2S8, Canada.
E-mail addresses: Joan.Wither@uhnresearch.ca (J.E. Wither), Alexander.Marson@ucsf.edu (A. Marson), Chris.Allen@ucsf.edu (C.D.C. Allen).
[1] Authors contributed equally.
[2] Present address: Building for Transformative Medicine, 60 Fenwood Rd., Brigham and Women's Hospital, Boston, MA 02115, USA.

https://doi.org/10.1016/j.jim.2018.03.009
Received 10 January 2018; Received in revised form 24 March 2018; Accepted 26 March 2018
Available online 31 March 2018
0022-1759/

engineered to secrete GLP-1 as a treatment for obesity in mice (Yue et al., 2017).

The components of CRISPR-Cas9 can be delivered in multiple ways, including viral transduction. Electroporation of Cas9 ribonucleoproteins (RNPs), comprised of synthetic guide RNA (gRNA) and Cas9 protein, has emerged as a method for high efficiency editing in primary human T cells (Schumann et al., 2015). RNP assembly does not require molecular cloning, which allows this approach to be readily scaled into a high-throughout, arrayed platform (Hultquist et al., 2016). In addition, electroporation obviates the need for viral production and stable genomic integration of CRISPR components, thereby simplifying experimentation and offering potential safety benefits for eventual clinical applications.

B cells present an attractive platform for genetic editing given their involvement in numerous autoimmune and infectious diseases (Granholm and Cavallo, 1992). One report described targeting of the immunoglobulin heavy chain locus in order to enforce class switching in mouse B cells and immortalized human-derived B cell lines (Cheong et al., 2016), while another used targeted gene knockouts to study V(D)J recombination in mouse pro-B cell lines (Lenden Hasse et al., 2017). Other studies have demonstrated the ability to generate high-efficiency gene knockouts in primary mouse B cells expressing a Cas9 transgene (Chu et al., 2016, 2017). Extension of these CRISPR-based editing techniques to primary human B cells has clear applications. While most research studies of B cells have been conducted in model systems or cell lines, use of CRISPR could enable detailed molecular and mechanistic studies of primary human B cells, providing valuable new insights into molecular function that may be relevant to human disease. B cells have also received minimal attention as a platform for therapeutic genetic manipulation, in contrast to T cells, of which engineered cell therapies are already clinically approved (Bach et al., 2017; Neelapu et al., 2017). Given the critical role of the B cell in humoral immunity, the vast range of potential peptide and non-peptide specificities conferred by the B cell receptor, and its ability to act at a distance via secretion of soluble immunoglobulin (LeBien and Tedder, 2008), engineered B cell therapies would have broad potential applications.

To achieve genetic manipulation of primary human B cells, we developed a methodology to deliver CRISPR-Cas9 RNPs by electroporation to B cells isolated from human peripheral blood or tonsils. We demonstrated genetic editing in experimental conditions reflecting a wide range of biological B cell states via application to two distinct in vitro culture systems, one which retained B cells in an undifferentiated state via co-culture with feeder cell lines, and another which permitted analysis of differentiating B cells that had been activated with soluble factors. We ablated single or even multiple genes at once by delivering appropriately targeted RNPs, and we additionally confirmed efficient editing at both genomic and protein expression levels. Finally, we demonstrated knock-in editing of a targeted gene by introducing a single-stranded DNA oligonucleotide (ssODN) template for homology directed repair (HDR) (Lin et al., 2014). Taken together, our findings establish a methodology for CRISPR-Cas9-based editing of primary human B cells, which will allow for experimental and therapeutic genomic editing of the humoral immune system.

2. Materials and methods

2.1. Stromal cell lines

A stable BAFF/CD40L-expressing OP9 cell line (OP9-BAFF/CD40L) was generated by a retroviral transduction approach using a CD40L-P2A-BAFF containing plasmid in a similar fashion to the CD40L-expressing OP9 cell line described previously (Oppermann et al., 2016). The pGEM-T plasmid containing human CD40L cDNA (NM_000074.2) and the pMD18-T plasmid containing human BAFF cDNA (NM_006573.3) were purchased from Sino Biological Inc. The CD40L coding region (excluding the stop codon) was amplified via PCR, with the addition of a 5′ *Bgl*II restriction site and a partial P2A linker at the 3′ site, using the following primers: forward 5′-cg gaa ttc AGA TCT ATG ATC GAA ACA TAC AAC CAA ACT TC-3′; reverse 5′- C CTC CAC GTC TCC AGC CTG CTT CAG CAG GCT GAA GTT AGT AGC TCC GCT TCC GAG TTT GAG TAA GCC AAA GG-3′. The BAFF coding region was amplified using the partial P2A linker sequence at the 5′ site and a *Bam*HI site at the 3′ site using the following primers: forward 5′-CTG CTG AAG CAG GCT GGA GAC GTG GAG GAG AAC CCT GGA CCT ATG GAT GAC TCC ACA GAA AGG-3′; reverse 5′-gcg tcg GGA TCC TCA CAG CAG TTT CAA TGC AC-3′. Both products were purified and joined in a PCR reaction using the flanking primers. The CD40L-P2A-BAFF product and the pMIY2 retroviral expression construct with an IRES EYFP reporter downstream of the cloning site were digested using BglII and BamHI and then ligated, and the correct sequence was verified. Retrovirus was generated by transfection of 293 T cells with Effectene (Qiagen) and a mixture of pMIY2-CD40L-P2A-BAFF and the GAG/Pol and VSV packaging plasmids. The medium was replaced at 24 h and collected at 48, 72, and 96 h. The virus-containing medium was filtered and then used to transduce low-passage OP9 bone marrow stromal cells (ATCC-CRL2749). OP9 cells that were positive for YFP and therefore infected with the retrovirus were stained with an anti-CD40L-PE antibody (Clone 24–31, Biolegend) were sorted using a FACS Aria II cell sorter (BD). OP9 or OP9-BAFF/CD40L cells were cultured in Alpha-MEM media (Invitrogen) supplemented with 20% fetal bovine serum (FBS, Wisent).

2.2. Human B cell isolation and culture

2.2.1. Peripheral blood B cell isolation and culture

Healthy human subjects between the ages of 18 and 40 years with no family history of autoimmune disease were recruited with approval by the Research Ethics Board of the University Health Network and informed consent of all subjects for collection of human peripheral blood samples. Peripheral blood mononuclear cells (PBMCs) were isolated via Ficoll-Paque Plus (GE Healthcare) gradient centrifugation following vendor instructions, and residual RBCs were lysed (RBC lysis buffer, Biolegend). Cells were washed once with 10% RPMI (Sigma) at room temperature. Primary B cells were negatively isolated from PBMCs using a Human B Cell Isolation Kit II (Miltenyi) following vendor instructions. Isolated B cells were rested in complete RPMI consisting of RPMI 1640 (Sigma) supplemented with 10% FBS (Wisent), L-glutamine (Gibco), non-essential amino acids (Gibco), and penicillin-streptomycin (Gibco) for up to 1 h at room temperature while RNPs were prepared (see below). Following electroporation, B cells were plated onto the OP9 or OP9-BAFF/CD40L stroma.

2.2.2. Tonsil B cell isolation and culture

Human tonsil samples were obtained from donors undergoing routine tonsillectomies through a protocol approved by the UCSF Human Research Protection Program and Institutional Review Board. Samples were deidentified upon collection and subsequent studies were considered not human subjects research according to the guidelines from the UCSF Institutional Review Board.

Tonsillar tissue was mechanically dissociated using scissors in phosphate-buffered saline (PBS, Gibco) containing 0.5 μg/ml amphotericin B (Sigma-Aldrich), then passed over a 40 μm nylon cell strainer. From this suspension, mononuclear cells were enriched by Ficoll gradient centrifugation in accordance with vendor-supplied instructions. Briefly, 15 ml of Ficoll-Paque PLUS (GE Life Sciences) media was added to a SepMate-50 conical tube (Stemcell Technologies), and 30 ml of tonsillar cell suspension were carefully layered on top. SepMate tubes were centrifuged at 1200 × *g* at room temperature for 10 min, and the top layer was poured into a new 50 ml conical tube. Leftover cells above the SepMate insert were scraped off using a sterile pipette tip and collected as well. Cells were washed three times with PBS, resuspended in a 9:1 by volume mixture of FBS (Gibco) and dimethyl sulfoxide

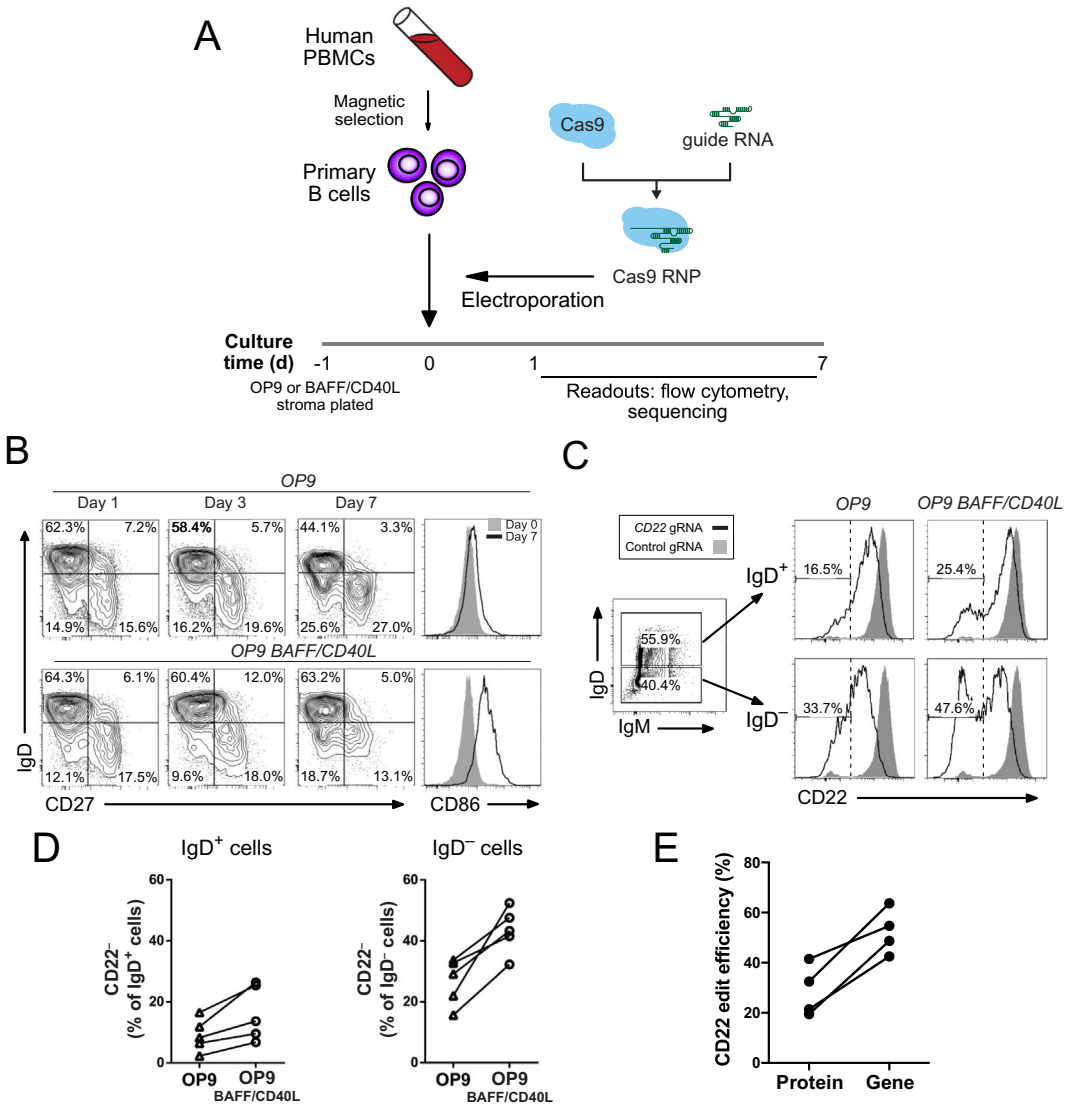

Fig. 1. CRISPR-Cas9 editing in primary human B cells with stromal cell co-culture. (A) Schematic representation of Cas9-gRNA RNP delivery to primary B cells isolated from human peripheral blood. B cells were cultured with OP9 or OP9-BAFF/CD40L cells following electroporation of RNPs. (B) Representative flow cytometry of IgD and CD27 (left) or CD86 (right) expression in primary human peripheral blood mononuclear cell (PBMC)-derived B cells co-cultured with OP9 or OP9-BAFF/CD40L cells. (C) Representative flow cytometry of CD22 expression in IgD^+ (top) or IgD^- (bottom) B cells co-cultured with OP9 or OP9-BAFF/CD40L following electroporation of RNPs targeting CD22 (black) or scrambled control (grey, filled). (D) Quantification of $CD22^-$ cells as a percentage of IgD^+ (left) and IgD^- (right) cells co-cultured with OP9 or OP9-BAFF/CD40L following electroporation with RNPs targeting CD22. (E) Quantification of editing efficiency as assessed by frequency of $CD22^-$ cells ("Protein") or frequency of reads containing indels centered on the predicted site of CD22 gRNA cut site ("Gene"). Each paired dot represents a single donor. B cells were co-cultured with OP9-BAFF/CD40L for 7 days following electroporation with RNPs targeting CD22.

(DMSO) at a cell density of 50 million cells per ml for cryopreservation.

B cells were subsequently isolated from cryopreserved aliquots using the Dynabeads Untouched Human B cells kit (Thermo Fisher Scientific) following vendor instructions, then resuspended in complete Iscove's modified Dulbecco's medium (IMDM) consisting of IMDM with GlutaMAX (Gibco) supplemented with 10% FBS (Gibco), 1 × penicillin-streptomycin (UCSF CCF), 0.25 μg/ml amphotericin B (Sigma-Aldrich), 100 U/ml Nystatin (Sigma-Aldrich), 50 μM 2-mercaptoethanol (Thermo Fisher Scientific), and 1 × Insulin-Transferrin-Selenium (Gibco). Cells were cultured in 96 well U-bottom plates (Corning) at a density of 100,000 cells in 200 μl volume per well and stimulated with 100 ng/ml anti-CD40 antibody (Clone G28.5, Bio-X-Cell) and 20 ng/ml recombinant human IL-4 (Peprotech) for 48 to 72 h prior to electroporation.

2.3. Assembly of ribonucleoprotein (RNP) complexes

Assembly of RNPs was performed as previously described (Schumann et al., 2015). Briefly, for experiments depicted in Fig. 1, pre-annealed complexes of CRISPR-targeting RNA (crRNA) and *trans*-activating crRNA (tracrRNA) were obtained at 40 μM from Synthego and mixed with 40 μM recombinant *Streptococcus pyogenes* Cas9 (UC Berkeley QB3 Macrolab) to form RNPs at 20 μM. In experiments depicted in Figs. 2 and 3, chemically synthesized crRNA and tracrRNA (IDT and Dharmacon) at concentrations of 160 μM were mixed and incubated at 37 °C for 30 min to form guide RNA (gRNA) at a concentration of 80 μM. Next, this gRNA was mixed in a 1:1 ratio by volume with 40 μM Cas9 and incubated at 37 °C for 15 min to form RNPs at a concentration of 20 μM. The selection of target sequences to maximize on-target and minimize off-target binding was aided by the web applications Deskgen and Benchling.

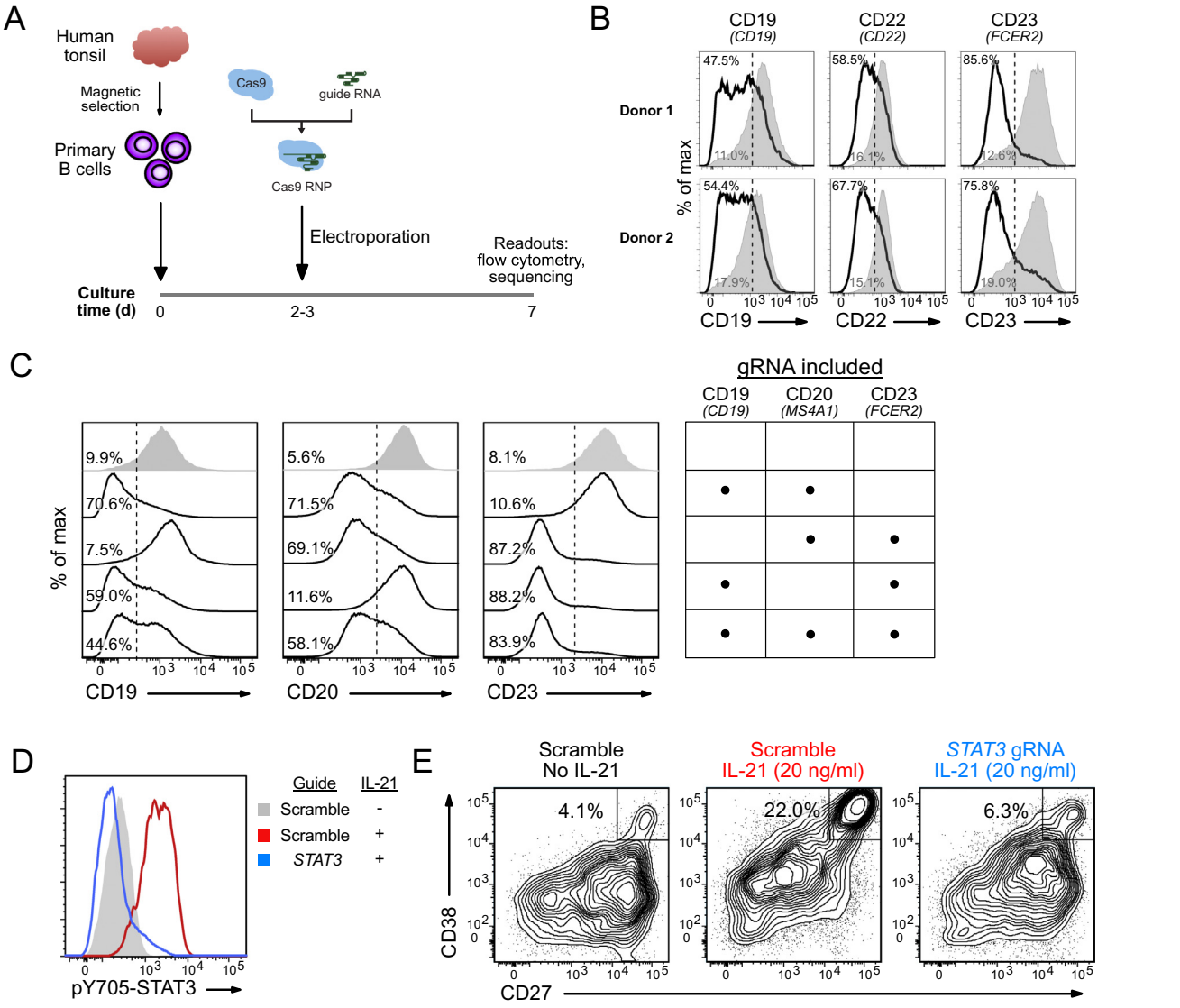

Fig. 2. Efficient and multiplexed CRISPR-Cas9 editing in ex vivo activated primary human B cells. (A) Schematic representation of RNP delivery to primary B cells isolated from human tonsil. B cells were cultured with anti-CD40 and IL-4 for 2 to 3 days preceding electroporation of RNPs formed by incubating Cas9 with appropriate crRNAs and tracrRNAs in vitro, then cultured for an additional 4 days with anti-CD40 and IL-4 before analysis. (B) Representative flow cytometry of surface molecule expression following electroporation of Cas9 RNPs targeting the specified genes (black) or scrambled control (grey, filled). (C) Representative flow cytometry (left) of CD19, CD20, and CD23 surface expression on B cells following electroporation of Cas9 RNPs simultaneously targeting multiple genes. Each row corresponds with the specified mix of Cas9 RNPs targeting the genes marked (•) in the table (right). (D) Representative flow cytometry of intracellular anti-phospho-STAT3 antibody staining in B cells following electroporation of RNPs targeting STAT3 (blue) or scrambled control (red) in the presence or absence (grey, filled) of IL-21. (E) Frequency of $CD38^{hi}CD27^{hi}$ plasma cells among B cells that received RNPs targeting STAT3 or scrambled control in the absence or presence of IL-21.

2.4. Primary B cell electroporation

B cells were pooled and resuspended in P3 buffer (Lonza) and added to 16-well Nucleocuvette Strips (Lonza). All experiments depicted in this study utilized cell densities ranging from 1 to 3×10^6 cells in a volume of 20 µl per reaction, which was found to be optimal, though editing was achieved at a lower bound of 3×10^5 cells/reaction. To each reaction, 2 to 5 µl of RNPs at 20 µM were added, with or without 1 µl of 100 µM HDR template (Table S1). For all experiments depicted in Fig. 2, a control HDR template with no homology to the human genome (Table S1) was added to increase Cas9 editing efficiency (Richardson et al., 2016). Nucleocuvette Strips were loaded into an Amaxa 4D Nucleofector (Lonza) and electroporated using the EH-115 (for Fig. 1) or EH-140 (for Figs. 2 and 3) pulse codes.

2.5. Post-electroporation B cell culture

For experiments depicted in Fig. 1, B cells were resuspended in complete RPMI with 20% FBS for 30 min prior to plating onto 24-well plates that had been pre-seeded with OP9 or OP9-BAFF/CD40L stromal cells overnight at a density of 50,000 cells per well in complete RPMI. For experiments depicted in Figs. 2 and 3, B cells were resuspended in complete IMDM prior to plating onto 96-well plates. Each reaction was split into 6 wells and resuspended in a final volume of 200 µl per well containing 100 ng/ml anti-CD40 and 20 ng/ml IL-4.

2.6. Flow cytometry

For experiments depicted in Fig. 1: Cell suspensions were stained with antibodies (Table S3) in PBS containing 2% FBS and 0.1% NaN_3

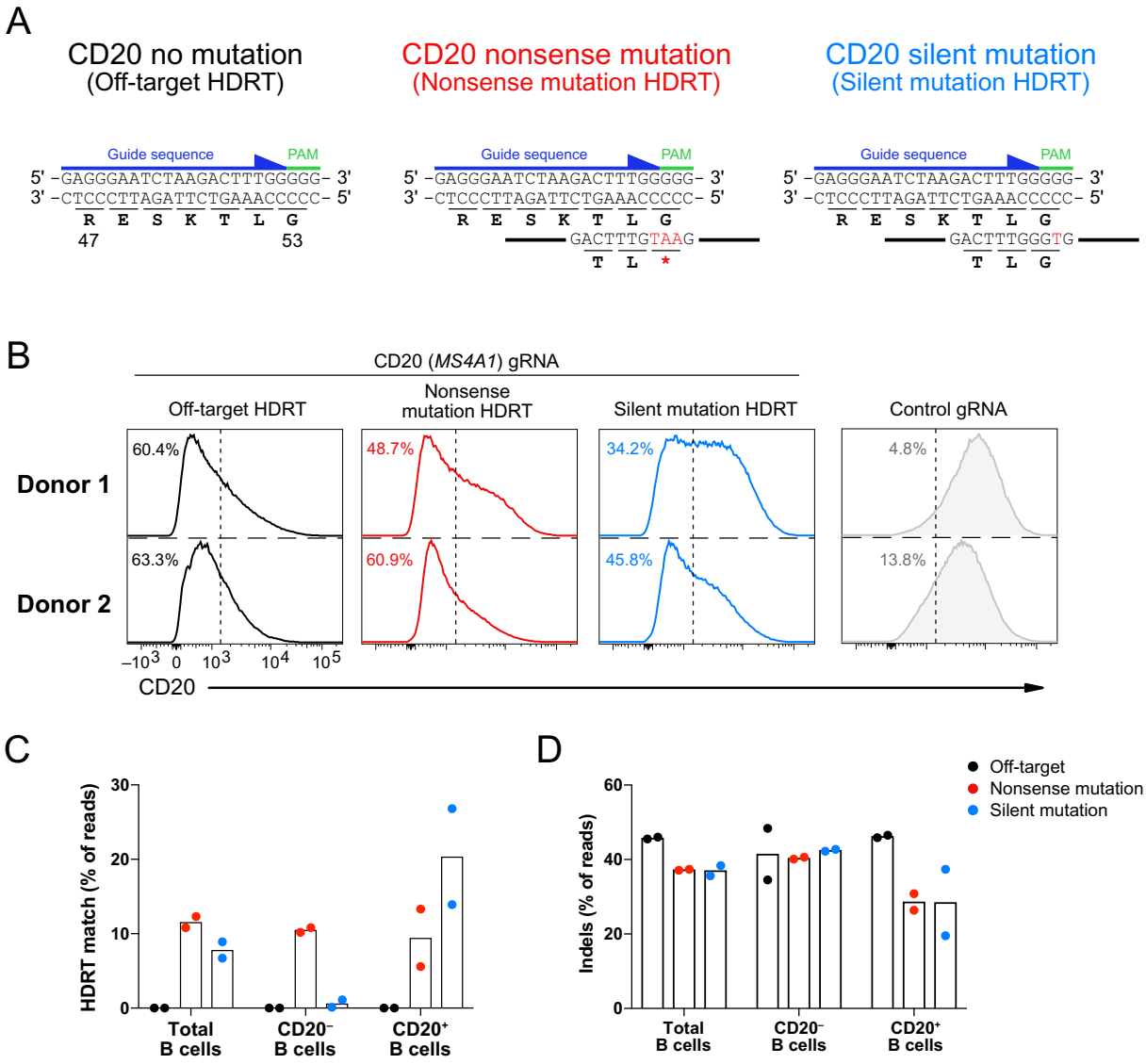

Fig. 3. Homology directed repair in primary human B cells. (A) Schematic representation of single-stranded CD20 HDR templates with 62 nt homology arms introducing nonsense or silent mutations at the protospacer adjacent motif (PAM, green). (B–D) B cells were cultured with anti-CD40 and IL-4 for 3 days prior to electroporation of RNPs targeting the *MS4A1* gene, along with HDR templates introducing nonsense (red) or silent (blue) mutations, or containing an irrelevant sequence (off-target, black), or a scrambled control RNP (grey), then cultured for an additional 4 days with anti-CD40 and IL-4 before analysis (B) or cell sorting (C–D). (B) Representative flow cytometry of surface CD20 expression in B cells following electroporation. Percentages represent the frequency of $CD20^-$ cells. (C) Frequency of reads recovered from total, $CD20^+$, and $CD20^-$ B cells that match the HDR template sequence. (D) Frequency of reads recovered from total, $CD20^+$, and $CD20^-$ B cells that contain indel mutations centered on the predicted gRNA cut site. Each dot represents a single donor. Donors represented in (B) are distinct from those represented in (C–D).

for 30 min on ice. Propidium iodide was used to exclude nonviable cells. Flow cytometry data were collected on a FACS Canto II (BD) and analyzed with FlowJo v9.

For experiments depicted in Figs. 2 and 3: Cell suspensions were stained with antibodies (Table S3) diluted in flow buffer consisting of PBS with 2% FBS, 1 mM EDTA, and 0.1% NaN_3 for 20 min on ice. Nonviable cells were excluded by labeling with fixable viability dye eFluor780 (eBioscience) during surface staining as described (Yang et al., 2012). To detect intracellular phosphorylated STAT3, cells were fixed in a final concentration of 2% (v/v) paraformaldehyde at room temperature for 10 min, then permeabilized in ice cold 90% methanol added dropwise, before staining with anti-pY705 STAT3-Alexa Fluor 647 (BD Bioscience) at room temperature for 30 min. Cells were washed twice with flow buffer between all steps. Flow cytometry data were collected on an LSR Fortessa (BD) and analyzed with FlowJo v10. All samples were gated on FSC-A versus SSC-A over a broad range of FSC-A to include blasting lymphocytes, followed by FSC-W versus FSC-H and then SSC-W versus SSC-H gates to exclude doublets.

2.7. IL-21 stimulation

To assay plasma cell differentiation, post-electroporation B cells were cultured in the presence of 100 ng/ml anti-CD40, 20 ng/ml IL-4, and 20 ng/ml recombinant human IL-21 (Peprotech) for 5 days. To assay STAT3 phosphorylation, B cells that had been cultured in the presence of anti-CD40 and IL-4 for 3 to 4 days following electroporation were washed and resuspended in PBS containing fixable viability dye eFluor780 (eBioscience) at a 1/600 dilution and incubated for 10 min at 37 °C to label nonviable cells. The cells were then washed and re-suspended in 100 µl of complete IMDM with or without 20 ng/ml IL-21 and incubated for 30 min at 37 °C before harvesting for flow cytometric analysis as described above.

2.8. Amplicon sequencing

Genomic DNA was isolated from either bulk or sorted primary human B cells as indicated in Fig. 3. Fluorescent activated cell sorting was performed using a FACS Aria II cell sorter (BD). 50,000 cells for each condition were sorted into 2.0 ml non-stick polypropylene tubes containing 100 µl of FBS and pelleted by centrifugation at 500 ×*g* for 5 min. After aspirating the supernatant, the cell pellet was resuspended in 20 µl of Quickextract DNA Extraction Solution (Epicenter) to a concentration of 2500 cells/µl. Genomic DNA in Quickextract was heated to 65 °C for 6 min and then 98 °C for 2 min, according to the manufacturer's protocol. 2 µl of the mixture, containing genomic DNA from 5000 cells, was used as template in a two PCR amplicon sequencing approach using NEB Q5 2X Master Mix Hot Start Polymerase with the manufacturer's recommended thermocycler conditions. After an initial 14 cycle PCR reaction with primers (Table S2) amplifying an approximately 200 bp region centered on the predicted gRNA cut site, a 1.0× SPRI purification was performed. A 6-cycle PCR to append P5 and P7 Illumina sequencing adaptors and well-specific barcodes was performed with 1 ng of purified PCR product as template, followed again by a 1.0× SPRI purification. Concentrations were normalized across wells, wells were pooled, and the library was sequenced on an Illumina MiniSeq with a 2 × 150 bp reads run mode. FASTQ files from indexed amplicon sequencing of gRNA cut sites were demultiplexed, and editing outcomes in each sample were individually analyzed using the CRISPResso analysis package (Pinello et al., 2016) with default parameters.

3. Results

3.1. Targeted knockout in undifferentiated human B cells with Cas9 RNPs

We sought to achieve CRISPR-Cas9-mediated gene knockouts in undifferentiated B cells. A two-component guide RNA (gRNA) consisting of a chemically synthesized CRISPR-targeting RNA (crRNA) complementary to exon 1 of the gene *CD22* and *trans*-activating crRNA (tracrRNA) was complexed with recombinant *Streptococcus pyogenes* Cas9 to form an RNP, which was then introduced via electroporation to primary B cells freshly isolated from human peripheral blood (Fig. 1A). Since primary B cells rapidly undergo apoptosis when cultured in isolation in the absence of stimulatory factors, we devised a co-culture system with a feeder cell line. Specifically, we stably expressed the pro-survival and activation factors BAFF (Mackay and Browning, 2002) and CD40L (Elgueta et al., 2009) in OP9 stromal cells (OP9-BAFF/CD40L) and compared these to the parent OP9 cell line in co-culture with B cells. Under both conditions, many B cells retained a naive-like IgD^+CD27^- phenotype, while a separate population of more activated, isotype-switched IgD^- cells also emerged (Fig. 1B). Electroporation of *CD22*-targeting RNPs yielded a population of cells lacking CD22 surface expression, consistent with successful targeted gene knockout (Fig. 1C).

Although in some cases over 20% of naïve IgD^+ B cells showed loss of surface CD22 following CRISPR-Cas9 targeting, greater knockout efficiency was seen in B cells with an IgD^- phenotype (Fig. 1D). When B cells were electroporated with RNPs targeting *CD19*, a similar trend toward increased CD19 knockout efficiency was also observed among IgD^- cells when compared with IgD^+ cells (Fig. S1A), suggesting activated cells may be more amenable to Cas9-mediated editing. In keeping with a potential role for activation status in gene editing efficiency, B cells that were co-cultured with OP9-BAFF/CD40L stroma exhibited on average a higher frequency of CD22 loss when compared with OP9 (Fig. 1C,D). Culture of B cells with OP9-BAFF/CD40L stroma did not lead to substantial changes in the frequency of cells expressing IgD or CD27, but likely induced some degree of cellular activation as evidenced by upregulation of the marker CD86 (Kohm et al., 2002) (Fig. 1B), again supporting the notion that activation renders cells more susceptible to Cas9-mediated editing.

Overall, delivery of RNPs targeting *CD22* led to surface protein loss in all donors and correlated with the percentage of alleles with insertion/deletion (indel) mutations as assessed by amplicon sequencing (Fig. 1E). Similar to findings in other cell types (van Overbeek et al., 2016), the spectrum of indels induced by the *CD22*-targeting RNP was largely conserved across donors (Fig. S2). Loss of surface CD22 increased as B cells were cultured for a longer time interval (Fig. S1B), consistent with a requirement for protein turnover in order for genomic changes to be reflected in surface protein expression.

3.2. Efficient gene knockout in ex vivo activated human B cells

While the ability to generate targeted genetic edits in primary human B cells with a naïve phenotype holds great research promise, we noted that efficiency of editing was greatest in activated cells. We therefore anticipated that in vitro activation of B cells prior to editing would lead to efficient genetic manipulation of differentiating B cells, permitting exploration of a different range of biological questions. We used an ex vivo culture system in which human tonsil-derived B cells were cultured with soluble activation factors anti-CD40 antibody and IL-4 prior to RNP electroporation (Fig. 2A). CD40L and IL-4 are signals provided to B cells by activated T cells in a T-dependent humoral immune response and promote both class switch recombination (Hasbold et al., 1998) and terminal differentiation into antibody-secreting plasma cells (Maliszewski et al., 1993). Activation with anti-CD40 and IL-4 for 3 days followed by electroporation of RNPs resulted in robust, high-efficiency knockout in a variety of surface proteins, including CD19, CD22, and CD23 (Fig. 2B). Magnitude of effects varied among donors and gene targets, likely due to heterogeneity in cell proliferation, levels of protein expression among starting cell populations, and protein turnover, but ranged from 45% to 85% knockout efficiency, with an average of 65%. Simultaneous electroporation of multiple RNPs with gRNAs targeting the indicated genes also permitted highly effective multiplexed knockout (Fig. 2C), with only slightly reduced editing efficiency in cells that received up to three distinct RNPs.

In order to test if Cas9-mediated gene editing could be linked to functional changes in B cell responses, we targeted a signaling pathway downstream of the cytokine IL-21, which induces phosphorylation of the transcription factor STAT3 (Avery et al., 2008). Cells receiving an RNP targeting the *STAT3* gene exhibited loss of phosphorylated STAT3 in response to IL-21, as would be expected in the case of STAT3 knockout (Fig. 2D). We also sought to test whether loss of STAT3 would have functional effects on B cells. IL-21 induces differentiation of B cells into plasma cells (PCs) in a STAT3-dependent manner (Deenick et al., 2013). We observed that *STAT3* knockout led to a roughly 4-fold reduction in the frequency of PCs in the presence of IL-21 (Fig. 2E), demonstrating the ability to observe a relevant phenotype caused by Cas9-mediated ablation of an intracellular protein.

3.3. Knock-in editing with a homology-directed repair template

While electroporation of Cas9 RNPs results in disruption of a targeted gene largely as a result of indels introduced by non-homologous end joining (NHEJ), introduction of an HDR template allows for knock-in editing of specific nucleotides (Schumann et al., 2015). To test this knock-in editing approach, we targeted the gene *MS4A1*, which encodes the protein CD20, using a combination of an RNP and one of three ssODN HDR templates (HDRTs). These HDRTs would 1) target a non-homologous genome sequence (an off-target control), 2) convert a glycine codon at amino acid 53 to a stop codon (a nonsense mutation), or 3) introduce a synonymous mutation that also disrupts the protospacer adjacent motif (PAM) sequence to preclude repeat cutting by Cas9 (a silent mutation) (Fig. 3A).

By flow cytometry, we observed that inclusion of an HDRT encoding a nonsense mutation led to minimal change or a slight reduction in the frequency of $CD20^-$ cells compared to an off-target control HDRT (Fig. 3B). When we then sorted $CD20^+$ and $CD20^-$ cells and sequenced

the *MS4A1* locus, we observed that the nonsense mutation was present in approximately 10% of reads, in both $CD20^+$ and $CD20^-$ cells (Fig. 3C). In contrast, the rates of indel mutations at the gRNA cut site were much higher than the frequency of HDR and were similar regardless of HDRT used (Fig. 3D). These findings suggested most cells that had undergone HDR were heterozygotes, carrying the targeted mutation on one allele and either an indel or no mutation on the other.

The inclusion of an HDRT encoding a silent mutation resulted in a smaller proportion of cells becoming $CD20^-$ compared with the off-target or nonsense mutation HDRTs (Fig. 3B). Sequencing revealed the silent mutation was present in approximately 20% of reads from $CD20^+$ cells but was nearly undetectable in $CD20^-$ cells, as expected (Fig. 3C). In summary, introduction of HDRTs led to knock-in editing at the *MS4A1* gene locus with efficiency exceeding 10% and could be correlated with noticeable changes in total surface protein expression.

4. Discussion

In this study, we demonstrated programmable CRISPR-Cas9 RNP-mediated editing in primary human B cells isolated from peripheral blood or tonsils. Multiple genes could be knocked out via simultaneous RNP introduction with minimal impact on editing efficiency, and ablation of a gene could also be correlated with a functionally relevant phenotypic change. Additionally, we demonstrated knock-in editing with efficiency exceeding 10% via the introduction of HDR templates. Together, these data indicate that primary human B cells can be directly modified at a genetic level without the need for viral vectors, permitting a broader range of experimental and therapeutic applications than has thus far been available to researchers.

In order to demonstrate that RNP electroporation is suited for diverse lines of biological inquiry, two distinct culture systems representing undifferentiated and actively differentiating B cells were tested in the course of this study; both were found to be highly compatible with Cas9 RNP electroporation. RNP electroporation carries an additional advantage in terms of scalability – all gRNA sequences in this study were synthetically defined and RNPs delivered in microtiter plate format. Though not directly explored in this study, the methodology we describe here could readily be adapted to a high-throughput, plate-based assay.

Some challenges remain, however. When we introduced specific mutations by HDRT, we found that these targeted mutations were present in about 10–20% of cells, whereas indel mutations occurred much more frequently, as has been observed in other studies (Cong et al., 2013; Platt et al., 2014; Paquet et al., 2016). Our results also suggested that the majority of HDR mutations were heterozygous, whereas only a small population of cells were likely to be homozygous for the targeted mutation. A method to mark the specific cells that have gained indel mutations versus HDR edits would therefore be of great value in functional studies, in order to detect phenotypes that may be subtle at a bulk population level but are enriched in subpopulations carrying specific mutations of interest.

The RNP electroporation approach we describe here is most effective in the context of introducing indels and targeted point mutations, due to current limitations in the size of commercially synthesized ssODNs to within a range of 200 to 400 bp (Wiles et al., 2015; Hung et al., 2017). Viral transduction approaches, on the other hand, would likely be most effective in situations requiring delivery of large HDR payloads or gene insertions, as has been demonstrated in a number of human cell types (Khan et al., 2011; Kabadi et al., 2014). While a direct comparison of the relative efficiencies of RNP electroporation and viral transduction approaches is difficult given inherent procedural differences, the RNP electroporation approach certainly offers advantages in terms of ease of handling and throughput, given the lack of cloning and viral assembly steps required.

As our study was being finalized, another group reported success using CRISPR-Cas9 RNPs in human B cells strongly activated in a multi-stage culture to induce plasma cell differentiation (Hung et al., 2017). This report further emphasizes the utility of RNP delivery as a viable method for CRISPR-Cas9 targeting in primary human lymphocytes. A distinction of our approach is that we provide methods for CRISPR-Cas9 targeting in B cells maintained in an undifferentiated state, as well as in B cells activated with a more limited set of stimuli to induce class switch recombination and plasma cell differentiation in a subset of cells. The protocols we described here require only a single culture step, simplifying experimental design and execution. Results from both studies suggest that higher efficiencies of protein modification following CRISPR-Cas9 targeting are likely to be observed with stronger stimulation of B cells. However, for some experiments or therapeutic approaches targeting undifferentiated B cells, strong activation may be contraindicated and thus our methodology may provide additional unique advantages.

In summary, RNP electroporation represents a versatile method of CRISPR-Cas9 delivery that can be used to study B cells in a variety of biological states, provides added ease and safety in comparison to viral transduction, and is amenable to high-throughput experimental formats. We anticipate that RNP-mediated genomic editing in primary human B cells can be readily applied to a diverse range of scientific questions and ultimately B cell-based cellular therapeutics.

Supplementary data to this article can be found online at https://doi.org/10.1016/j.jim.2018.03.009.

Funding

This work was supported by the University of California, San Francisco Sandler Asthma Basic Research Center and the National Institute of Allergy and Infectious Diseases of the National Institutes of Health [Grant Number R01AI130470] (C-A.M.W. and C.D.C.A.), as well as a the Canadian Institutes of Health Research [Grant Number PJT-148948] (J.E.W.). C-A.M.W. receives support from the Howard Hughes Medical Institute Medical Research Fellows and University of California, San Francisco Pathways to Discovery programs. C.D.C.A. is a Pew Scholar in the Biomedical Sciences, supported by The Pew Charitable Trusts. A.M. holds a Career Award for Medical Scientists from the Burroughs Wellcome Fund and is a Chan Zuckerberg Biohub Investigator. J.E.W. receives salary support from the Arthritis Centre of Excellence. The content is solely the responsibility of the authors and does not necessarily represent the official views of the funding agencies.

Author contributions

C-A.M.W., T.L.R., Y.B., D.M.F., P.B., J.C.Z-P., J.E.W., A.M., and C.D.C.A. designed research and analyzed data; C-A.M.W., T.L.R., and Y.B. performed research; J.E.W., A.M., and C.D.C.A. supervised research; K.W.R. provided tonsil samples; and C-A.M.W., T.L.R., Y.B., J.E.W., A.M., and C.D.C.A. wrote the manuscript.

Competing financial interests statement

A.M. is a cofounder of Spotlight Therapeutics and serves as an advisor to Juno Therapeutics and PACT Therapeutics. The Marson lab has received sponsored research support from Juno Therapeutics and Epinomics. Intellectual property has been filed on Cas9 RNP delivery methods by the Marson lab. The Allen and Wither labs declare no competing financial interests.

References

Avery, D.T., et al., 2008. STAT3 is required for IL-21-induced secretion of IgE from human naive B cells. Blood 112 (5), 1784–1793.
Bach, P.B., Giralt, S.A., Saltz, L.B., 2017. FDA approval of tisagenlecleucel: promise and complexities of a $475000 cancer drug. JAMA 318 (19), 1861–1862.
Barrangou, R., Doudna, J.A., 2016. Applications of CRISPR technologies in research and beyond. Nat. Biotechnol. 34 (9), 933–941.

Cheong, T.C., Compagno, M., Chiarle, R., 2016. Editing of mouse and human immunoglobulin genes by CRISPR-Cas9 system. Nat. Commun. 7, 10934.
Chu, V.T., et al., 2016. Efficient CRISPR-mediated mutagenesis in primary immune cells using CrispRGold and a C57BL/6 Cas9 transgenic mouse line. Proc. Natl. Acad. Sci. U. S. A. 113 (44), 12514–12519.
Chu, V.T., Graf, R., Rajewsky, K., 2017. CRISPR/Cas9-mediated in vitro mutagenesis in GC-like B cells. Methods Mol. Biol. 1623, 135–145.
Cong, L., et al., 2013. Multiplex genome engineering using CRISPR/Cas systems. Science 339 (6121), 819–823.
Deenick, E.K., et al., 2013. Naive and memory human B cells have distinct requirements for STAT3 activation to differentiate into antibody-secreting plasma cells. J. Exp. Med. 210 (12), 2739–2753.
Elgueta, R., et al., 2009. Molecular mechanism and function of CD40/CD40L engagement in the immune system. Immunol. Rev. 229 (1), 152–172.
Granholm, N.A., Cavallo, T., 1992. Autoimmunity, polyclonal B-cell activation and infection. Lupus 1 (2), 63–74.
Hasbold, J., Lyons, A.B., Kehry, M.R., Hodgkin, P.D., 1998. Cell division number regulates IgG1 and IgE switching of B cells following stimulation by CD40 ligand and IL-4. Eur. J. Immunol. 28 (3), 1040–1051.
Hultquist, J.F., et al., 2016. A Cas9 ribonucleoprotein platform for functional genetic studies of HIV-host interactions in primary human T cells. Cell Rep. 17 (5), 1438–1452.
Hung, K.L., et al., 2017. Engineering protein-secreting plasma cells by homology-directed repair in primary human B cells. Mol. Ther. 26 (2), 456–467.
Kabadi, A.M., Ousterout, D.G., Hilton, I.B., Gersbach, C.A., 2014. Multiplex CRISPR/Cas9-based genome engineering from a single lentiviral vector. Nucleic Acids Res. 42 (19), e147.
Khan, I.F., Hirata, R.K., Russell, D.W., 2011. AAV-mediated gene targeting methods for human cells. Nat. Protoc. 6 (4), 482–501.
Kohm, A.P., Mozaffarian, A., Sanders, V.M., 2002. B cell receptor- and beta 2-adrenergic receptor-induced regulation of B7-2 (CD86) expression in B cells. J. Immunol. 168 (12), 6314–6322.
LeBien, T.W., Tedder, T.F., 2008. B lymphocytes: how they develop and function. Blood 112 (5), 1570–1580.
Lenden Hasse, H., et al., 2017. Generation and CRISPR/Cas9 editing of transformed progenitor B cells as a pseudo-physiological system to study DNA repair gene function in V(D)J recombination. J. Immunol. Methods 451, 71–77.
Lin, S., Staahl, B.T., Alla, R.K., Doudna, J.A., 2014. Enhanced homology-directed human genome engineering by controlled timing of CRISPR/Cas9 delivery. elife 3, e04766.
Lombardo, A., Naldini, L., 2014. Genome editing: a tool for research and therapy: targeted genome editing hits the clinic. Nat. Med. 20 (10), 1101–1103.
Long, C., et al., 2014. Prevention of muscular dystrophy in mice by CRISPR/Cas9-mediated editing of germline DNA. Science 345 (6201), 1184–1188.
Mackay, F., Browning, J.L., 2002. BAFF: a fundamental survival factor for B cells. Nat. Rev. Immunol. 2 (7), 465–475.
Maliszewski, C.R., et al., 1993. Recombinant CD40 ligand stimulation of murine B cell growth and differentiation: cooperative effects of cytokines. Eur. J. Immunol. 23 (5), 1044–1049.
Neelapu, S.S., et al., 2017. Axicabtagene ciloleucel CAR T-cell therapy in refractory large B-cell lymphoma. N. Engl. J. Med. 377 (26), 2531–2544.
Oppermann, S., et al., 2016. High-content screening identifies kinase inhibitors that overcome venetoclax resistance in activated CLL cells. Blood 128 (7), 934–947.
van Overbeek, M., et al., 2016. DNA repair profiling reveals nonrandom outcomes at Cas9-mediated breaks. Mol. Cell 63 (4), 633–646.
Paquet, D., et al., 2016. Efficient introduction of specific homozygous and heterozygous mutations using CRISPR/Cas9. Nature 533 (7601), 125–129.
Pinello, L., et al., 2016. Analyzing CRISPR genome-editing experiments with CRISPResso. Nat. Biotechnol. 34 (7), 695–697.
Platt, R.J., et al., 2014. CRISPR-Cas9 knockin mice for genome editing and cancer modeling. Cell 159 (2), 440–455.
Richardson, C.D., Ray, G.J., Bray, N.L., Corn, J.E., 2016. Non-homologous DNA increases gene disruption efficiency by altering DNA repair outcomes. Nat. Commun. 7, 12463.
Schumann, K., et al., 2015. Generation of knock-in primary human T cells using Cas9 ribonucleoproteins. Proc. Natl. Acad. Sci. U. S. A. 112 (33), 10437–10442.
Schwank, G., et al., 2013. Functional repair of CFTR by CRISPR/Cas9 in intestinal stem cell organoids of cystic fibrosis patients. Cell Stem Cell 13 (6), 653–658.
Wiles, M.V., Qin, W., Cheng, A.W., Wang, H., 2015. CRISPR-Cas9-mediated genome editing and guide RNA design. Mamm. Genome 26 (9–10), 501–510.
Yang, Z., Sullivan, B.M., Allen, C.D., 2012. Fluorescent in vivo detection reveals that IgE (+) B cells are restrained by an intrinsic cell fate predisposition. Immunity 36 (5), 857–872.
Yue, J., Gou, X., Li, Y., Wicksteed, B., Wu, X., 2017. Engineered epidermal progenitor cells can correct diet-induced obesity and diabetes. Cell Stem Cell 21 (2), 256–263 (e254).
Zhen, S., et al., 2015. Harnessing the clustered regularly interspaced short palindromic repeat (CRISPR)/CRISPR-associated Cas9 system to disrupt the hepatitis B virus. Gene Ther. 22 (5), 404–412.